www.amlett.org, www.amlett.com, DOI: 10.5185/amlett.2012.icnano.157
"ICNANO 2011" Special Issue Published online by the VBRI press in 2012

Comparative study of TiO_2 and $TiSiO_4$ nanoparticles induced oxidative stress and apoptosis of HEK-293 cells

Ramovatar Meena[1], Ruchita Pal[2] , Surya Narayan Pradhan[1], Madhu Rani[1] and R. Paulraj[1]*

[1]*School of Environmental Sciences, Jawaharlal Nehru University New Delhi, India*
[2]*Advanced Instrumentation Research Facility, Jawaharlal Nehru University New Delhi, India*

*Corresponding author. Tel: (+91) 11-2670 4162; E-mail: paulrajr@hotmail.com

ABSTRACT

The aim of this study is to compare the cyto and genotoxic effects of TiO_2 and $TiSiO_4$ nanoparticles on human embryonic kidney cells (HEK-293). The cell viability, induction of oxidative stress, and cell apoptosis induction were assessed after 48 h of cell exposure to TiO_2 and $TiSiO_4$ nanoparticles separately. Our results showed that nanoparticles induce the generation of reactive oxygen species (ROS) followed by significant depletion of glutathione levels and increased lipid peroxidation. The cells exhibited apoptotic morphology like condensed chromatin and nuclear fragmentation after 48 h of treatment. Both the particles induce oxidative stress and DNA damage in a dose dependent manner. Oxidative stress is the underlying mechanism by which nanoparticle causes DNA damage and apoptosis. This study further indicate that TiO_2 nanoparticles has more toxic effects than $TiSiO_4$ nanoparticles on HEK cells, which demonstrate that larger size may be responsible for retardant of cellular uptake. This might be reducing the toxicity of $TiSiO_4$ nanoparticles.

Keywords: TiO_2 nanoparticle; cytotoxicity; oxidative stress; cell apoptosis.

Ramovatar Meena is a Senior Research Fellow (CSIR) in the School of Environmental Sciences, Jawaharlal Nehru University, New Delhi. He is pursuing his Ph.D. under supervision of Dr. Paulraj Rajamani. He has received B.Sc. (Agri. Hons) from Maharana Pratap University of Agricultural Sciences, Udaipur and M.Sc. (Agri. Biotechnology) from Marathwada Agriculture University, Parbhani, Maharashtra, India. His field of research is Nanoparticles synthesis and their biomedical applications. Presently he is working on in-vitro and in-vivo effects of various metal oxide nanoparticles. He has published more than 5 papers in the reputed International Journals.

Paulraj Rajamani obtained his Ph.D. degree in Environmental Sciences from Jawaharlal Nehru University, New Delhi. He is appointed as assistant professor in the School of Environmental Sciences, Jawaharlal Nehru University, New Delhi. He received Young scientist award from International Union of Radio Science General Assembly, Canada. Dr. Paulraj is a reviewer of many journals. His research interest includes Synthesis and Application of Nanomaterials, Nano risk assessment, bioelectromagnetics, cancer biology and Environmental occupational health.

Introduction

The revolution in nanotechnology brings advantages in diverse areas of our lives such as engineering, information-technology and medicine, etc. However, recent studies also suggested that nano-materials with their nano size (0.1–100 nm) could easily enter into the human body **[1-2**]. The small size and high surface-volume ratio endowed them with an active group or intrinsic toxicity [**3-5**]. Rationally the widespread application of nanoproducts would arise the concerns about the nano-thing risk on human being health because of their size and high reactive surface, totally differing from their bulk materials **[6**].

Titanium dioxide nanoparticles (nano-TiO_2) are widely used in the cosmetics, pharmaceutical, and paint industries as a coloring material because of its high stability, anticorrosion and photocatalytic properties **[7-10].** TiO_2 NPs have also been shown to produce reactive oxygen species (ROS) leading to the toxicity **[9, 11-13]** TiO_2 nano anatase besides having photo-catalytic activity also induced oxidative DNA damage, lipid peroxidation, micronuclei formation, and increased hydrogen peroxide and nitric oxide production in a human bronchial epithelial cell line in the absence of light **[11]** However, very few studies have reported the toxic effects of nanoparticles. Pereira et al 2010, [**14**] shows that aqueous suspensions of $TiSiO_4$, were responsible for the mutagenic potential for TA98 and TA100 strains of Salmonella typhimurium, after 30 days of

soil incubation. The instability of $TiSiO_4$ NPs after 2h of soil incubation may have been responsible for their availability to yield toxic effects on Salmonella typhimurium (TA100).

Earlier studies have shown that Titanium particles induce apoptosis in different types of cells, such as mesenchymal stem cells [**15**], osteoblasts [**16**], brain cells [**17**], and necrosis in fibroblasts [**18**]. Recently, it has been shown that ultrafine TiO_2 can cause cyto and genotoxicity and induce apoptosis in human lymphoblastoid cells [**9**]. Still, there is little information on the patterns of cell death induced specifically by titanium nanoparticles. Therefore, the objective of the present study is to compare the cytotoxicity and induction of apoptosis by TiO_2 and $TiSiO_4$ nanoparticles in HEK-293 with following objectives: (a) To evaluate whether nanoparticles are capable of inducing cytotoxicity and genotoxicity in human embryonic kidney cells, (b) To observe the link between nanoparticles induced oxidative stress and cell apoptosis.

Experimental

Materials

Titanium dioxide nanoparticles (TNPs) and Titanium silicon oxide (TSNPs), MTT [3-(4,5-dimethythiazoyl-2-yl) 2,5-diphenyl tetrazolium bromide), RNase, proteinase K, low melting point agarose (LMPA), DMSO (dimethyl sulfoxide), triton-X-100, Propidium iodide (PI), EDTA (Ethylene diamine tetraacetic acid), pyrogallol, glutathione reduced, NADPH (Nicotinamide adenine dinucleotide phosphate), TCA (Trichloroacetic Acid), TBA (Thiobarbituric acid) were purchased from Sigma-Aldrich-USA. Dulbecco's Modified Eagle's Medium (DMEM), (FCS) fetal calf serum and IX Penstrep antibiotic solution were purchased from Biological Industries, Isreal. Rest of chemicals was purchased from local chemical company.

Experimental cell line

Human embryonic cell line (HEK-293) , obtained from National Centre for Cell Science (NCCS) Pune was cultured in Dulbecco's Modified Eagle's Medium, supplemented with 10% heat inactivated Fetal calf serum and IX Penstrep antibiotic solution and incubated at 37ºC and 5% CO_2.

Characterization of nanoparticles

The nanoparticles were characterized by transmission electron microscopy (TEM), X-ray diffraction (XRD) and dynamic light scattering (DLS). TNPs and TSNPs (50µg/ml) were dissolved in distilled water and ultrasonicated for 30 min to make the homogeneous suspension. After sonication, the sample was prepared by placing a drop of homogeneous suspension on a copper grid with a laser carbon film and allowing it to dry in air. TEM images were observed with a JEOL-JEM-2100F TEM operating at 200 kV. The diameters of randomly selected particles were measured at 15,000 × magnification, and the elemental analysis was done using an energy-dispersive x-ray analyzer (EDX). The hydrodynamic diameters of nanoparticles were evaluated by DLS. Samples were loaded into a sample holder and DLS data were collected by using a Malvern DLS apparatus (Nano-ZS, Malvern Instruments, Malvern, UK) with a 633 nm He/Ne laser.

Cytotoxicity assay

MTT (tetrazolium salt) assay was applied to evaluate the effect of TNPs and TSNPs on HEK-293 cells viability by measuring the uptake and reduction of tetrazolium salt to an insoluble formazan dye by cellular microsomal enzymes [**19**]. The exponentially growing cells (about105cells/well) were seeded into 96-well culture plates and incubated with various concentrations (50, 100, 150 and 200 µg/ml) of TNPs and TSNPs for 24, 48 and 72 h. Four hours before termination, the supernatants were substituted with 90µl fresh medium and 10µl of MTT (1 mg/ml) solution. After 4hr incubation at 37°C, the medium was aspirated and the formazan crystals were solubilized in 200µl DMSO. The absorbance was measured spectrophotometrically (Bio-Rad 840) at 570 nm.

All measurements were done in triplicates. The relative cell viability (%) related to control wells containing cells without nano-particles was calculated by

$$[A]_{exposure} / [A]_{control} \times 100$$

where, [A]exposure is the absorbance of the treated sample and [A]control is the absorbance of the control sample.

Oxidative stress

Intracellular ROS level was detected by using 2',7'-dichlorofluorescin diacetate (DCFH-DA), a non-polar compound, which could enter cells and be hydrolyzed into polar form 2',7'-dichlorodihydrofluorescein (DCFH) [**23**]. The intracellular DCFH is an oxidation sensitive fluorescent probe which could be oxidized by ROS to produce fluorescent 2', 7'-dichlorofluorescin (DCF). The fluorescence intensity of DCF was positive correlated with the intracellular ROS quantity. The Cells in logarithmic growth phase were incubated for 24 h, then the old medium was replaced with medium containing different concentration (50, 100, 150 and 200µg/ml) of nanoparticles for 48 h. After exposure, the cells were washed with phosphate-buffered saline (PBS), and then they were resuspended at a concentration of $1x10^6$ cells/ml and were stained with 40 µM DCFH-DA for 30 min. At the end of DCFH-DA incubation, cells were washed with PBS, lysed with NaOH, and aliquots were transferred to an eppendorf tube. The fluorescence intensities were measured by flow cytometry (FCM, Beckman-coulter), with an excitation wavelength of 488 nm and an emission wavelength of 525 nm.

Oxidative stress markers

After treating the cells for 48 h with different nanoparticle suspension (50-200 µg/ml), cells were washed with PBS, scraped, lysed, sonicated for 15 s on ice and centrifuged at 14,000 rpm for 15 min at 4°C. The supernatant (cell lysate) was removed and the protein concentration was measured by the Bradford method. The activities of different

oxidative stress marker enzymes were measured in the cell lysates.

SOD assay

Superoxide dismutase (SOD) activity was determined as per the method of Marklund [**21**]. SOD catalyses the dismutation of superoxide radical to yield hydrogen peroxide and oxygen. The assay is based on the ability to inhibit auto-oxidation of pyrogallol. The cell lysates containing 50µg protein were treated with triton-x-100 (1%) and kept at 4°C for 30 min followed by addition of 1 ml of assay mixture containing 0.05 M sodium phosphate buffer (pH 8.0), 0.01 M EDTA and 0.27 mM pyrogallol. The absorbance was measured for 5 min at 420 nm. Solution of pyrogallol was made in 100 mM HCl. The enzyme activity was expressed as U/mg protein, where 1U is the amount of enzyme required to bring about 50% inhibition of the auto-oxidation of pyrogallol.

Catalase assay

The activity of catalase enzyme was measured as previously described [**22**]. An appropriate volume of cell lysate containing 50 µg protein was mixed with 1 ml of 50 mM potassium phosphate buffer (pH 7.0) containing 10 mM H_2O_2 in 1 ml quartz cuvette. The decrease in absorbance of H_2O_2 was followed at 240 nm for 4 min. Catalase activity was calculated from the slope of the H_2O_2 absorbance curve and normalized to protein concentration.

GPx assay

The activity of glutathione peroxidase (GPx) was measured using 50 µg protein of the cell lysates. The cell lysates were mixed with tert-butyl hydroperoxide (30 mM), reduced glutathione (2 mM), Glutathione reductase (0.5 unit/ml) and NADPH (0.25 mM) in 50 mM Tris- HCl (pH 8) at 25°C. The decrease in NADPH absorbance was followed for 3 min at 340 nm. The activity of GPx was calculated from the slope of NADPH absorbance curve and was normalized to protein content.

LPx assay

Lipid peroxidase in microsomes was estimated spectrophotometrically by thiobarbituric acid reactive substances (TBARS) method as described by Varshney and Kale [**27**] and is expressed in terms of formation of malonaldehyde (MDA) per mg protein. In brief, 0.4 ml of microsomal sample was mixed with 1.6 ml of Tris- KCl (0.15M KCl + 10mM Tris-HCl, pH 7.4) buffer to which 0.5 ml of 30% TCA was added. Then 0.5 ml of TBA was added. The tubes were covered with aluminium foil and placed in a water bath for 45 min at 80ºC, cooled in ice and centrifuged at room temperature for 10 min at 3000 rpm in Remi-T8 table- top centrifuge. The absorbance of the clear supernatant was measured at 531.8 nm in spectrophotometer.

DNA damage assay

Cells were harvested and fixed with 1:3 glacial acetic acid/methanol and washed with phosphate buffered saline (PBS) (1.37mM NaCl, 4.3mM Na_2HPO_4, 2.7mM KCl, 1.4mM KH_2PO_4, pH 7.4). Single cell gel electrophoresis (SCGE) was performed as the method of Meena and Paulraj, [**24**]. Cellular DNA damage was visualized under fluorescence microscope (Carl Zeiss) after staining with a fluorescent DNA-binding dye Ethidium bromide (EtBr). 50 cells were randomly selected from each slide of different groups and the results were analyzed by Comet IV software.

Detection of apoptosis

The suspended single cells subjected to treatment with TNPs and TSNPs at different concentrations for 48 h were harvested. Cells were collected by combining floating and adherent cells, washed with PBS, centrifuged at 1200 rpm and fixed overnight in chilled methanol (-20ºC). After fixation, cells were washed with cold PBS and rehydrated for 30 min. The cells were incubated with RNase-A solution (50 mg/ml) for 20 min in dark. Finally propidium iodide (5 mg/ml) was added and samples were acquired by using the FACS CALIBUR flow cytometer (B.D. biosciences).

Statistical analysis

All experiments were repeated at least three times, and one representative from these experiments with similar results is shown. The quantitative data of continuous variables were expressed as mean ± SEM Statistical significance was tested by Student's t-test or ANOVA with post hoc analysis when appropriate. P value <0.05 was considered statistically significant.

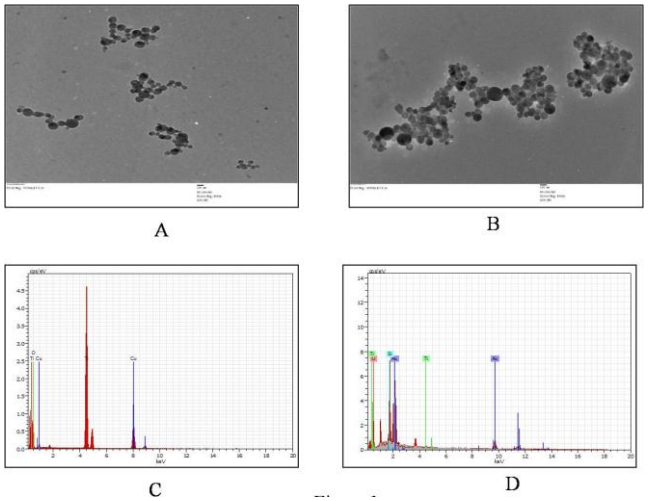

Fig. 1. TEM image (A) TiO_2 nanoparticles, (B) $TiSiO_4$ nanoparticle at 8000x magnification. The particle size was calculated with TEM ranges from 10–35 nm. Scale bar size is 200 nm. (C, D) Energy dispersive x-ray profile of TNPs and TSNPs respectively.

Results and discussion

Characterization of nanoparticles

TNPs were found in cluster form and average diameter was about 10- 20 nm (**Fig. 1a**). The wide-angle region of the X-ray diffraction (XRD) patterns of TNPs exhibited a high-

intensity diffraction peak at 2θ =25.2º and four additional peaks at 2θ = 37.7º, 48.0º, 54.7º and 62.5º (**Fig. 2a**) that were ascribed to 101, 004, 200, 211 and 002 diffractions of tetragonal TiO_2 respectively. Size of TNPs calculated on the basis of half angle and the height of peak with XRD was nearly equivalent to the size calculated by TEM (10±2 -25±2nm). The size of the TSNPs was determined by transmission electron microscopy, results show that the TSNPs also had cluster form and an average diameter of 15-35 nm (**Fig. 1b**). The wide-angle region of the X-ray diffraction patterns of TSNPs exhibited a high-intensity diffraction peak at 2θ =25.47º and three additional peaks at 2θ = 38.0º, 48.17º and 68.8º (**Fig. 2b**) with the respective size 15.3, 9.2, 7.3 and 10.4 nm. Size of TSNPs calculated by XRD and TEM was (5±1- 16±1 nm). The DLS results show the well distributed and steady state of TNPs and TSNPs in the prepared solution with an average size of 72.3 and 123.2 nm respectively (**Fig. 3**). These results indicates that

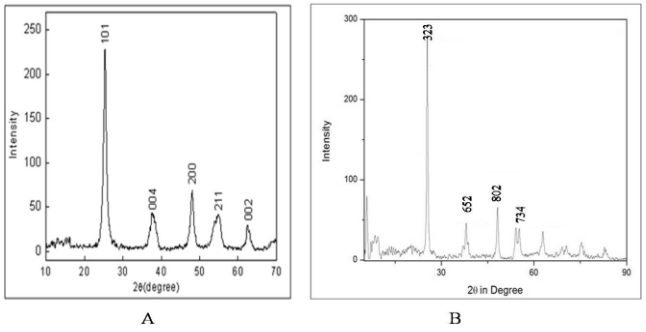

Fig. 2. Shows the powder X-ray diffraction patterns of TNPs and TSNPs with Miller indices (h k l) showing crystal family of planes for each diffraction peak.

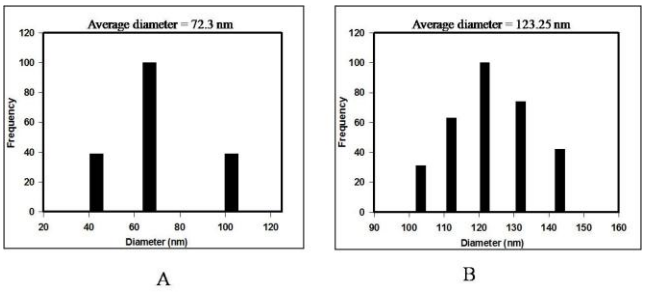

Fig. 3. Indicates the size distribution pattern of TNPs and TSNPs generated by dynamic light scattering (DLS).

Time course and dose-dependent cytotoxicity

HEK-293 cells were exposed to TNPs and TSNPs at 50, 100, 150 and 200 µg/ml dosage levels for 24 h, 48 h, and 72 h. Cell viability decreased as a function of both concentration and time (P<0.001). The dose dependent cell viabilities of TNPs treated cells at 24 h were 92.0%, 85.4%, 74.2% and 66.2%, followed by a reduction to 85.2%, 69.1%, 61.8% and 44.8% at 48 h exposure. After 72-h exposure, cell numbers had decreased to 79.1%, 63.3%, 47.3% and 32.7% as compared to the control. Whereas the cells treated with $TiSiO_4$ nanoparticle, shows a different kind of cell viability trend. Cell viability was not significantly decrease in 50 and 100µg/ml TSNPs treated cells (P>0.05). But the cell viabilities of 150 and 200µg/ml $TiSiO_4$ NPs treated cells were significantly decrease in a dose and time dependent manner (P<0.05). The dose dependent cell viabilities of TSNPs treated cells at 24 h were 96.5%, 94.3%, 82.8% and 83.1%, followed by a reduction to 93.4%, 78.2%, 76.3% and 74.2% at 48 h exposure. After 72-h exposure, cell numbers had decreased to 91.6%, 77.6%, 69.3% and 58.4%, compared to the control (**Fig. 4**).

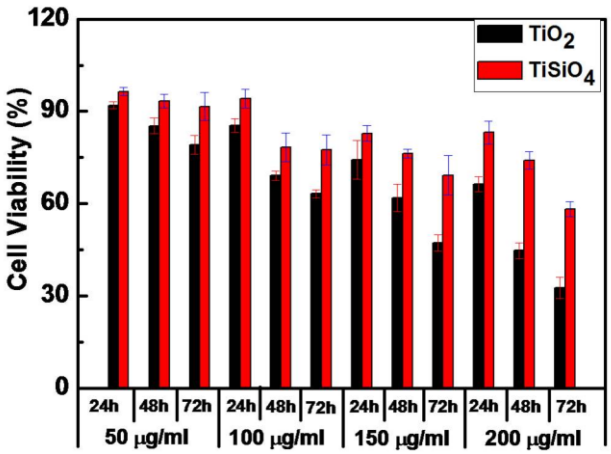

Fig. 4. Shows cell viability of HEK-293 cells after exposure to 50, 100 and 200 mg/L of TNPs and TSNPs for 24, 48 and 72 h. Data are expressed as Mean ± S.D. *indicates p < 0.05 compared with control group.

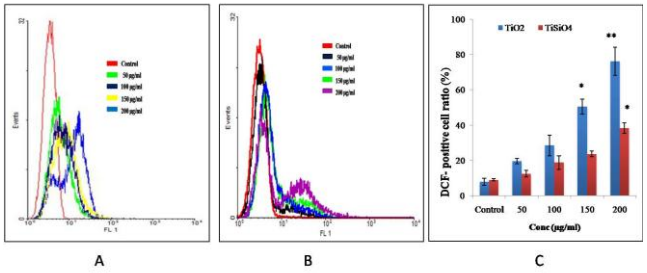

Fig. 5. (A) Histogram represents data from DCF-DA staining for detecting reactive oxygen species production in the TNP treated HEK -293 cells. The *x* axis represents the fluorescence intensity, and the *y* axis represents the number of cells collected (10000 cells) (B) Reactive oxygen species production in the TSNP treated HEK -293 cells. (C) The graph represents the percent of gated cells for DCF-DA staining.

Cellular oxidative stress and lipid peroxidation

DCF fluorescence intensity, an indicator of oxidative stress (OS) in the cells, increased after 48-h exposure to TNPs and TSNPs at all examined concentrations. The Oxidative stress level of TNPs treated cells was higher as compare to TSNPs treated cells. The number of DCF positive cells was increased more significantly (19.5%, 28.4%, 50.5 % and 76.1%) after exposure of TNPs (P<0.001). Whereas the cells treated with TSNPs, the DCF positive cells were not increased significantly in a dose dependent manner (12.5 %, 17.3%, 23.7% and 33.2%) (**Fig. 5**).

Cellular SOD level exhibited a dose-dependent decrease. Compared to control, the SOD levels were decreased 5.31%, 21.3%, 40.5% and 63.5% after exposure to respective dose of TNPs (**Fig. 6a**). Whereas the cellular SOD level of TSNPs treated cells were reduced significantly by 25.5% and 30.5% of control only at the concentration of 150 and 200 µg/ml ($p<0.05$).There was a significant negative correlation between ROS levels and SOD levels in both TNPs and TSNPs treated cells (R2 =0.943 and 0.927 respectively). The Catalase activity also decreased in a dose dependent manner (**Fig. 6b**). Compared to control, the Catalase levels were decreased 5.31%, 21.3%, 40.5% and 63.5% after exposure to respective dose of TNPs. While, catalase level of TSNPs treated cells were reduced significantly by 31.2% of control only at the concentration of 200 µg/ml ($p<0.001$).

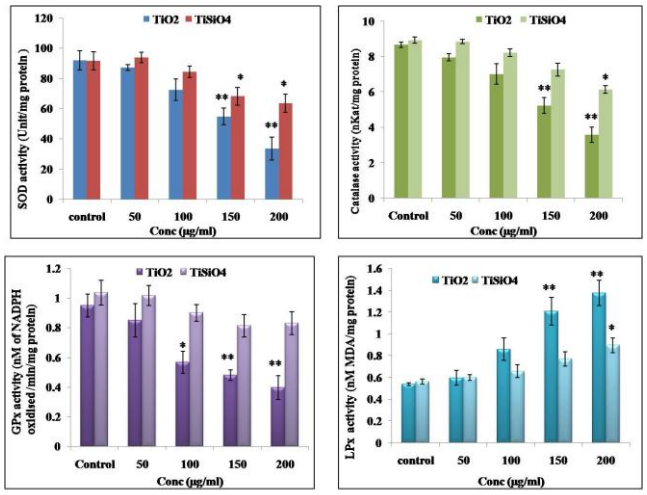

Fig. 6. Shows the comparison of antioxidative enzyme level among the control and nanoparticles (TNPs and TSNPS) treated HEK-293 cells. (A) SOD activity (Unit/mg protein), (B) Catalase activity (nKat/mg protein), (C) GPx activity (nM of NADPH oxidised/min/mg protein), (D) LPx activity (nM MDA/ mg protein).

Cellular GPx level exhibited also a dose-dependent decrease (**Fig. 6c**). The GPx levels were reduced significantly by 10.5%, 41.5%, 49.4% and 59% as compared to control, after 48h exposure to TNPs at the four exposure levels ($p<0.001$). Whereas the cellular GPx level of TSNPs treated cells were reduced significantly by 21.2% and 22.4% of control only at the concentration of 150 and 200 µg/ml ($p<0.05$). There was a significant negative correlation between ROS levels and GPx levels in both TNPs and TSNPs treated cells. (R2 =0.986 and 0.968 respectively).

The cell membrane damage was reflected in the elevated MDA levels in the cell medium after cells were exposed to TNPs and TSNPs for 48 h (**Fig. 6d**). The cells treated with TNPs show that MDA level were elevated significantly by 0.59±0.06, 0.85±0.10 and 1.20±0.11 and 1.37±0.11 nM/mg protein at the four respective exposure levels compared to the control groups 0.53±0.01 ($p<0.01$). But cellular MDA level was not significantly increased in TSNPs treated cells in a dose dependent manner ($p>0.001$). There was a significant correlation between ROS levels and MDA levels in TNPs treated cells. (R^2 =0.966).

Nanoparticles induced DNA Damage

The DNA Damage induced by TNPs and TSNPs were measured by comet assay. The extensive and dose-dependent damage to DNA was observed in TiO_2 nanoparticle treated groups. The 100-200 µg/ml TNPs treated cells showed very high rate of DNA damage, the comet length was increased significantly as compared to control group. But the lower concentration of TNPs did not induce DNA damage in HEK-293 cells (**Fig. 7a-d**). A significant increase in DNA damage of HEK-293 cells treated with 200µg/kg of TSNPs was observed. The results illustrate that the intensity of DNA damage in TNPs was less as compared to TSNPs (**Fig. 7e-h**).

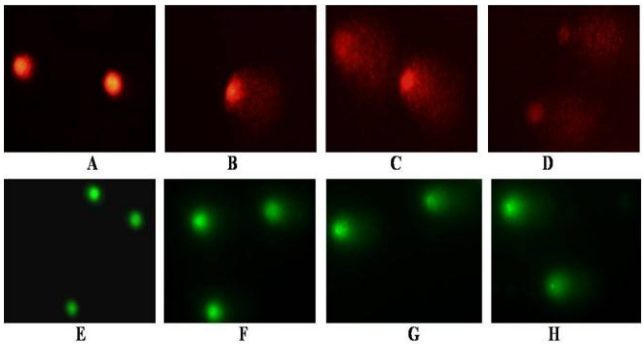

Fig. 7. DNA strand breaks of HEK-293 cells treated with different doses of TNPs and TSNPs. Image A-D indicates control, 50, 100 and 200µg/ml comet image of TNPs treated HEK-293 respectively. The E-H indicates control, 50, 100 and 200µg/ml images of the comet of HEK-293 cells treated with TSNPs.

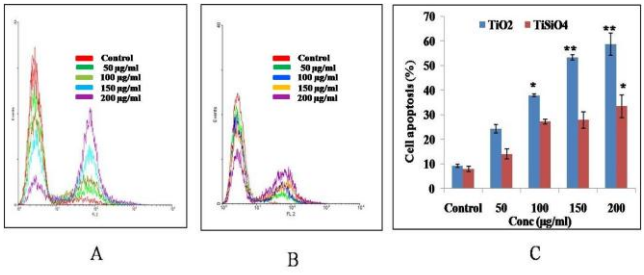

Fig. 8. Shows cell apoptosis HEK-293 cells among the nanoparticles (TNPs and TSNPs) treated groups and control group. (A) Overlay histograph of TNPs treated groups and control ones. X –axis shows number of events and y- axis indicate fluorescence at FL-2 log. (B) Overlay histograph of TSNPs treated groups and control group. (C) Shows the total apoptotic cells population of HEK-293 cells in percentage.

Nanoparticle induced apoptosis

TNPs and TNSPs both increased sub G1 hypodiploid cell population in a dose dependent manner. There were significant increase in apoptotic DNA content (24.2±1.6, 37.8±0.57, 53.3±1.4 and 58.6±4.4%) in TNPs treated groups as compared to control group (9.18±0.61%) ($p<0.001$). The cells treated with 50µg/ml TSNPs did not show any significant change in apoptotic DNA content with respect to control groups, But higher concentration of TSNPs (100-200µg/ml) causes significant increase in cell apoptosis in dose dependent manner (27.1±0.9, 27.8±3.4 and 33.4±4.5%) (**Fig. 8**). The linear relationship between

the ROS level and the cell apoptosis indicated that free radical species were generated by exposure to TNPs and TSNPs which increases number of apoptotic cells (R^2 = 0.974 and 0.930, respectively). All these result support the notion that TNPs induces cell apoptosis in HEK cells in a dose dependent manner, whereas in nano $TiSiO_4$ treated cells, the cell apoptosis pattern was not in a dose dependent manner.

In the present study, it was found that exposure to TiO_2 nanoparticles at dosage levels of 50–200 µg/ml caused both dose- and time-dependent cytotoxicity as revealed by MTT assay. While the treatment of $TiSiO_4$ nanoparticle at similar doses did not induce dose dependent cytotoxicity, only higher doses (150 and 200 µg/ml) caused significant cytotoxicity as compared to control groups. Our results are consistent with a study of Adams et al [**25**], they investigated the potential eco-toxicity of nanosized titanium dioxide (TiO_2), silicon dioxide (SiO_2), and zinc oxide (ZnO) water suspensions using Gram-positive Bacillus subtilis and Gram-negative Escherichia coli as test organisms and observed that SiO_2 was the least toxic of the nanomaterials tested and relatively high concentrations were required to achieve a reduction in cell growth. Behar [**30**], also studied that cell viability following exposure to 400 µg/cm^2 SiO_2 and Fe_2O_3 remained unchanged; these particles were non-toxic to HEp-2 cells. In case of TiO_2 nanoparticles treated cells, the cellular oxidative stress was manifested by elevated ROS levels, reduced GSH and SOD levels, and increased catalase and lipid peroxidation. The inverse linear relationship between the ROS level and the GSH, SOD level indicated that free radical species were generated by exposure to TiO_2 nanoparticles which reduced intracellular antioxidant levels (R^2 = 0.986). Moreover, free radicals also resulted in the production of malondialdehyde, an indication of lipid peroxidation. There was a strong correlation between decreased cell viability and increased ROS level after 48 h exposure (R^2 = 0.995). Whereas, $TiSiO_4$ nanoparticle treated cells, only higher doses (150 and 200µg/ml) shows significant increase in ROS level and decrease in GSH, SOD and Catalase level. The significant correlation was observed between decreased cell viability and increased ROS level. (R^2= 0.952).

The reverse correlation between the decreased cell viability and the increased MDA suggested that cell death was the primary cause of the membrane damage by lipid peroxidation. Lactate dehydrogenase leakage form cells are another evidence for penetration of particles into the cells and cell membrane damage. It has been well documented that lactate dehydrogenase levels (as a marker of necrosis) in the cell medium elevated after the cells exposed to nanoparticles. Flow cytometric analysis showed that TiO_2 nanoparticles can increased the sub G1 hypodiploid cell population in a dose dependent manner. Where as in $TiSiO_4$ treated cells, cell apoptosis was not significantly increased in a dose dependent manner.

Conclusion

Thus results concluded that apoptosis initiated by titanium may be the result of increased ROS production and GSH depletion, leading to mitochondrial dysfunction, DNA damage and increased expression of apoptotic genes. The comparative data of TiO_2 and $TiSiO_4$ nanoparticles shows that at similar doses, $TiSiO_4$ has less cytotoxic and genotoxic effects compared to TiO_2 nanoparticles, it may be possible that larger size NPs has less cellular uptake, which might be reason for lower toxicity of $TiSiO_4$ nanoparticles. Further studies are needed to understand the changes in physiochemical properties of $TiSiO_4$ nanoparticles and its molecular mechanisms by which it induces toxicity.

Acknowledgment

Authors are thankful to Advance Instrumentation Research Facility (AIRF), JNU New Delhi for Transmission Electron Microscopy, Scanning Electron Microscope and Flow cytometer facility.

Reference

1. Kreyling, W.G.; Semmler, M.; Erbe, F.; Mayer, P.; Takenaka, S.; Schulz, H.; Oberdorster, G.; Ziesenis, A. *J. Toxicol. Environ. Health A.* **2002**, *65*, 1513-30. **DOI:** 10.1080/00984100290071649
2. Takenaka, S.; Karg, E.; Roth, C.; Schulz, H.; Ziesenis, A.; Heinzmann, U. *Environ. Health Perspect*. **2001**, *109*, 547–551. **DOI:** 10.1289/ehp.01109s4547
3. Hoet, P.H.; Bruske-Hohlfeld, I.; Salata, O.V. *J. Nanobiotechnol*. **2004**, *2*, 12. **DOI:** 10.1186/1477-3155-2-12
4. Donaldson, K.; Stone, V.; Gilmour, P.S.; Brown, D.M.; Macnee, W. *Phys. Eng. Sci*. **2000,** *358*, 2741-2749. **DOI:** 10.1098/rsta.2000.0681
5. Warheit, D.B. *Mater. Today*. **2004**, *7*, 32-35.
6. Donaldson, K.; Tran, C.L. *Inhal. Toxicol*. **2002**, *14*, 5-27. **DOI:** 10.1080/089583701753338613
7. Gelis, C.; Girard, S.; Mavon, A.; Delverdier, M.; Pailous, N.; Vicendo, P. 2003. *Photodermatol. Photoimmunol. Photomed*. **2003**, *19*, 242-253. **DOI:** 1034/j.16000781.2003.00045.x
8. Sun, D.; Meng, T.T.; Loong, H.; Hwa, T.J. *Water Sci. Technol.* **2004**, *49*, 103-110.
9. Gheshlaghi, Z.N.; Riazi, G.H.; Ahmadian, S.; Ghafari, M.; Mahinpour, R. *Acta Biochim. Biophys. Sin.* **2008**, *40*, 777-782. **DOI:** 10.1111/j.1745-7270.2008. 00458.x
10. Gurr, J.; Wang, A.A.S.; Chen, C.; Jan, K. *Toxicology*. **2005**, *213*, 66-73. **DOI:** 10.1016/j.tox.2005.05.007
11. Wang, J.J.; Sanderson, B.J.; Wang, H. *Mutat. Res.* **2007**, *628*, 99-106. **DOI:**10.1016/j.mrgentox.2006.12.003
12. Kang, S.J.; Kim, B.M.; Lee, Y.J.; Chung, H.W. *Environ. Mol. Mutagen*. **2008**, *49*, 399-405. **DOI:** 10.1002/em.20399
13. Barnard, A.S. *Nat. Nanotechnol*. **2010**, *5*, 271-274. **DOI:** 10.1038/nnano.2010.25
14. Pereira, R.; Rocha-Santos, T.A.P.; Antunes, F.E.; Rasteiro, M.G.; Ribeiro, R.; Gonçalves, F.; Soares, A.M.V.M.; Lopes, I.; *J. Hazard. Mater*. **2011,** *194*, 345-354**.** **DOI:**10.1016/j.jhazmat.2011.07.112
15. Wang, M.L.; Tuli, R.; Manner, P.A.; Sharkey, P.F.; Hall, D.J.; Tuan, R.S. *J. Orthopaed. Res.* **2003**, *21*, 697-707. **DOI:** 10.1016/S0736-0266(02)00241-3

16. Pioletti, D.P.; Takei, H.; Kwon, S.Y.; Wood, D.; Sung, K.L. 1999. *J. Biomed. Mater. Res.* **1999**, *46*, 399-407.

DOI:10.1002/(SICI)1097-4636(19990905)46:3<399::AID-JBM13>3.0.CO;2-B

17. Long, T.C.; Tajuba, J.; Sama, P.; Saleh, N.; Swartz, C.; Parker, J.; Hester, S.; Lowry, G.V.; Veronesi, B. *Environ. Health Perspect.* **2007**, *115*, 1631-1637.

DOI: 10.1289/ehp.10216

18. Osano, E.; Kishi, J.; Takahashi, Y. *Toxicol. In Vitro*. **2003**, *17*, 41-47.

DOI: 10.1016/S0887-2333(02)00127-3

19. Denizot, F.; Lang, R. *J. Immunol. Meth*. **1986,** *89*, 271-277.
DOI: 10.1016/0022-1759(86)90368-6

20. Elbekai, R.H.; El-Kadi, A.O.S. *Free Radic Biol Med*. **2005**, *39*, 1499-1511.

DOI:10.1016/j.freeradbiomed.2005.07.012

21. Marklund, S.L.; Marklund, G. *Eur. J. Biochem*. **1974**, *47*, 469-474.

DOI: 10.1111/j.14321033.1974.tb03714.x

22. Aebi, H. E. *Methods Enzymol*. **1984**, 121-126.

DOI: 10.1016/S0076-6879(84)05016-3

23. Varshney, R.; Kale, R.K. *Int. J. Rad. Biol*. **1990**, *58*, 733-743.

DOI: 10.1080/09553009014552121

24. Meena, R.; Paulraj, R. *Toxicol. Env. Chem*. **2012**, *94*, 146-163.
DOI: 10.1080/02772248.2011.638441

25. Adams, L.K.; Lyon, D.Y.; Alvare, J.J. *Water Res.* **2006**, *40*, 3527-3532.
DOI: 10.1016/j.watres.2006.08.004

26. Baher, F.; Stephania, A. C. *Toxicol. In Vitro.* **2009**, *23*, 1365-1371.
DOI: 10.1016/j.tiv.2009.08.005

27. Balduzzi, M.; Diociaiuti, M.; De Berardis, B.; Paradisi, S.; Paoletti, L. 2004. *Environ. Res*. **2004**, *96*, 62-71.

DOI: 10.1016/j.envres.2003.11.004

28. Sayes, C.M.; Gobin, A.M.; Ausman, K.D.; Mendez, J.; West, J.L.; Colvin, V.L. *Biomaterials*. **2005**, *26*, 7587-7595.

DOI:10.1016/j.biomaterials.2005.05.027

29. Hussain, S.M.; Hess, K.L.; Gearhart, J.M.; Geiss, K.T.; Schlager, J.J. *Toxicol. In Vitro*. **2005**, *19*, 975-983.

DOI: 10.1016/j.tiv.2005.06.034

30. Lin, W.S.; Huang, Y.W.; Zhou, X.D.; Ma, Y.F. *Toxicol. Appl. Pharmacol*. **2006,** *217*, 252-259.

DOI: 10.1016/j.taap.2006.10.004

